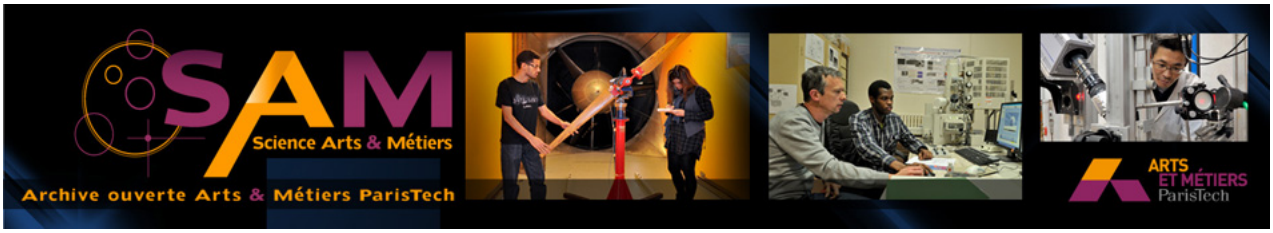

Investigation and comparative analysis of plastic instability criteria: application to forming limit diagrams

Farid Abed-Meraim · Tudor Balan · Guillaume Altmeyer

Abstract The prediction of forming limit diagrams (FLDs) is of significant interest to the sheet metal forming industry. Although a large variety of plastic instability criteria have been developed during the previous decades, there is still a lack of comparison of their respective theoretical bases. The aim of this paper is to present the theoretical formulations of a representative selection of diffuse necking and strain localization criteria based on the maximum force principle, the Marciniak–Kuczyński method and the bifurcation approach. The theoretical foundations and underlying assumptions for each criterion are specified prior to their application to several materials to determine the associated FLDs. The capability of the criteria to predict the formability of thin metal sheets is discussed and a classification of some of the criteria is attempted according to their order of occurrence in terms of the localization prediction.

Keywords Necking · Strain localization · Anisotropic elasto-plasticity · Large strain · Formability · Forming limit diagram

1 Introduction

The ability to predict the onset of necking and strain localization during sheet metal forming is important for the choice of the process that would avoid defective products. For stretched sheet metals, two forms of necking, diffuse and localized, may occur. It has been shown that diffuse necking appears prior to localized necking, and it is now well recognized that the maximum allowable strain in sheet metal forming is determined by localized necking. The concept of the forming limit diagram (FLD) is widely used to characterize the formability of thin metal sheets and to quantify the ductility of metallic materials. This idea was introduced by Keeler and Backofen for the experimental assessment of formability [1, 2]. Although standardized experimental FLD tests exist, the experimental determination of FLDs suffers from a lack of reproducibility, which can be partly attributed to high sensitivity of the FLDs to experimental factors. Moreover, these specific tests are restricted to simple geometries and remain expensive and time consuming. To overcome these drawbacks, theoretical methods to determine FLDs, based on the use of localization criteria, have been investigated for several decades. These contributions are based on various approaches, ranging from empirical observations to theoretically sound criteria, making them more or less general, applicable to various types of materials and able to predict diffuse necking or localization by shear bands.

Based on Considère's empirical observation, which found that diffuse necking began developing in a bar when the maximum force was reached during a tensile test [3], Swift [4] proposed an extension of this criterion to the biaxial tension of a sheet. This extension made the criterion applicable for the determination of diffuse necking in the expansion domain of the FLD. Concurrently, for the left hand side of the FLD, Hill [5] proposed another two-dimensional extension of Considère's criterion based on a maximum load criterion coupled with the occurrence of strain localization along a zero-extension rate band in the sheet plane. Because there is no zero-extension rate direction in the sheet plane for the stretching domain, the Hill'52 criterion is only applicable to the prediction of localized strains in the sheet plane for the left-hand side of the FLD. To predict strain localization for both sides of the FLD, Considère's criterion has been extended for biaxial loadings by Hora and coworkers [6] by including the

F. Abed-Meraim (✉) · T. Balan · G. Altmeyer
Laboratoire d'Étude des Microstructures et de Mécanique des Matériaux, LEM3, UMR CNRS 7239, Arts et Métiers ParisTech, Metz, 4 rue Augustin Fresnel, 57078 Metz, France
e-mail: farid.abed-meraim@ensam.eu

contribution of the minor principal strain; Mattiasson et al. [7] later included the effect of strain path evolution towards plane strain during the loading of the sheet. It should also be noted that additional formulations of this criterion are available, which are primarily aimed at refining the prediction of FLDs by considering more advanced material models and by including the effects of damage [8] or strain rate sensitivity [9].

Another important class of plastic instability criteria is based on the bifurcation theory. For this type of theoretical approach, necking can be viewed as a more or less rapid evolution from a homogeneous to a heterogeneous strain state. Plastic instability is then interpreted as a loss of uniqueness of the solution of the boundary value problem. Drucker [10] and then Hill [11] introduced a general condition for non-bifurcation that was based on the positiveness of the second-order work. This primarily diffuse necking criterion provides a lower bound and appears to be too conservative for the accurate prediction of FLDs in practical applications. By introducing a zero stress rate tensor condition, Valanis [12] proposed a less conservative variant of the previous criterion. Although this latter criterion is less conservative than the former, they provide equivalent FLD predictions in the case of small deformations and associative plasticity as they operate, in this particular case, on the same symmetric tangent modulus. For large strains and associative plasticity, which is the context of this paper, the relevant tangent modulus loses its symmetry; however, both criteria still provide nearly the same results for many FLD situations. Localization, in the form of shear or necking bands, can also be regarded as a discontinuity of certain mechanical fields across the localization band. Such localized modes can be recovered by Hill's general non-bifurcation criterion by introducing into the bifurcation problem a specific discontinuous form of the strain rate, i.e., a particular admissible form for the velocity gradient jump across the band. This leads to a localization criterion corresponding to the loss of ellipticity of the partial differential equations governing the boundary value problem, as subsequently described by Rice and coworkers [13–15]. The localization condition is reached when the acoustic tensor associated with the elastic–plastic tangent modulus becomes singular, which for associative plasticity and smooth yield surface requires softening. Such a situation can be reproduced either by adopting plasticity models with yield surface vertices, e.g., through the use of micromechanical modeling [16–18], or, as developed in this paper, by considering damage mechanisms. In addition to softening, it should also be noted that the applicability of these bifurcation-based criteria is restricted to strain rate-independent materials. For rate-sensitive materials, alternative approaches to the bifurcation theory have been proposed in the literature, e.g., the use of stability analysis [19–21].

A final category of localization prediction techniques is based on the existence of initial heterogeneities in the sheet metal. Originally, two distinct homogeneous areas were introduced: the so-called safe zone and the defect zone. The form of the initial imperfection can be either geometric, i.e., a band of reduced thickness [22], or heterogeneity in terms of the mechanical properties of the sheet [23]. Because no experimental work could properly establish the relationship between the postulated imperfection and the actual heterogeneities, the introduced imperfection should only be considered as an equivalent defect. The comparison of the evolution of mechanical and geometrical properties inside and outside the affected area allows the determination of the occurrence of localization during the loading of the metal sheet. A significant drawback of this method is the introduction of the initial thickness ratio as an arbitrary user-defined parameter. More recently, the development of efficient finite element methods and high performance computers has made it possible to extend this two-zone imperfection theory to multi-area problems. To avoid the issues related to the strong assumption made by Marciniak and Kuczyński for the definition of the form of the initial heterogeneity, this effect may be introduced as a random thickness distribution of a discretized metal sheet [24]. Similar to the approach of Marciniak and Kuczyński, localization is predicted when the strain concentrates into a local, narrow part of the sheet.

This non-exhaustive overview of necking and localization criteria reveals numerous approaches, based on various observations and theories. Nevertheless, comparisons of their theoretical bases as well as confrontations of their applications on a wide range of materials are still insufficiently developed for the assessment of their respective capability to accurately predict FLDs for new materials.

The main objectives of this paper are to present and discuss the theoretical foundations of the major localization criteria and to recast their mathematical formulations into a unified and more general modeling framework for the comparison of the corresponding predicted FLDs for a range of materials. After introducing in Section 2 a general material modeling framework based on a phenomenological approach, the formability criteria most widely used to predict FLDs are presented in Section 3. The foundations of the criteria rely on the Maximum Force Principle and the Marciniak–Kuczyński two-zone method. Section 4 is devoted to the plastic instability criteria that are based on the bifurcation approach. Starting from their mathematical formulations, an attempt is made to provide a classification of these necking criteria in terms of their conservative nature in the prediction of sheet metal formability. To support the discussed approaches and their classification, the implementation of the associated criteria coupled with phenomenological constitutive laws has been completed, and the results are compared for several materials. Finally, the main results and conclusions are summarized.

2 Constitutive modeling

The material modeling adopted in this work is based on a phenomenological approach, which allows for the description of the behavior of elastic–plastic materials with or without damage effects during the forming operations and, particularly, during the deep-drawing of sheet metals. Thermal and viscous effects that may occur during forming are not taken into account in this constitutive modeling that is restricted to cold deformations of non-viscous materials. The sheet metal is considered to be initially free from residual stresses, undamaged and homogeneous.

During forming, sheet metals are subject to large deformations. The associated kinematics are based on the multiplicative decomposition of the deformation gradient $\mathbf{F}$:

$$\mathbf{F} = \mathbf{F}^e \cdot \mathbf{F}^p \tag{1}$$

where $\mathbf{F}^e$ and $\mathbf{F}^p$ are the elastic and plastic parts of the deformation gradient, respectively. The total strain rate $\mathbf{D}$ and the total spin $\mathbf{W}$ are then obtained as the symmetric and skew-symmetric part, respectively, of the velocity gradient $\mathbf{G} = \dot{\mathbf{F}} \cdot \mathbf{F}^{-1}$.

Because sheet metals undergo large deformations and rotations during forming processes, the adequate constitutive framework requires the use of objective time derivatives. This can be achieved by writing the tensor variables of the constitutive laws in an orthogonal rotation-compensated frame. Choosing the orthotropic co-rotational frame, which is associated with the rotation of the continuum, the material time derivative in the co-rotational frame is linked to the Jaumann objective co-rotational derivative by a simple relationship. In the following paragraphs, constitutive laws are formulated in the co-rotational frame associated with the Jaumann objective derivative (see reference [25] for more details on the kinematics of large deformations, the choice of objective derivative, and its relation to the co-rotational frame).

2.1 Elastic–plastic model

The primary intended application of the current constitutive modeling is deep drawing; therefore, the elastic–plastic model accounts for the anisotropy of the sheet but is restricted to cold deformation. A hypo-elastic law describes the evolution of the Cauchy stress:

$$\dot{\boldsymbol{\sigma}} = \mathbf{C} : (\mathbf{D} - \mathbf{D}^p) \tag{2}$$

where $\mathbf{C}$ is the fourth-order elasticity modulus that links the Cauchy stress rate to the elastic part of the strain rate (in the co-rotational frame).

The plastic strain rate tensor is given by the following associative flow rule:

$$\mathbf{D}^p = \dot{\lambda} \frac{\partial F}{\partial \boldsymbol{\sigma}} = \dot{\lambda} \mathbf{V} \tag{3}$$

where $\dot{\lambda}$ and $\mathbf{V}$ are, respectively, the plastic multiplier and the flow direction, normal to the yield surface defined by the potential F. This potential defines the yield criterion and can be written under the Kuhn–Tucker form:

$$\begin{aligned} &F = \overline{\sigma}\left(\boldsymbol{\sigma}'\right) - Y \leq 0 \\ &\dot{\lambda} \geq 0 \\ &\dot{\lambda} F = 0 \end{aligned} \tag{4}$$

where $\boldsymbol{\sigma}'$ denotes the deviatoric part of the Cauchy stress tensor and Y measures the current size of the yield surface, whose evolution is related to isotropic hardening. Two classical yield functions $\overline{\sigma}$ are considered in this paper. The first one is the isotropic von Mises function

$$\overline{\sigma} = \sqrt{\frac{3}{2} \boldsymbol{\sigma}' : \boldsymbol{\sigma}'} \tag{5}$$

for which the flow direction is given by

$$\mathbf{V} = \frac{3}{2} \frac{\boldsymbol{\sigma}'}{\overline{\sigma}} \tag{6}$$

The second one is the anisotropic Hill'48 quadratic function:

$$\overline{\sigma} = \sqrt{\boldsymbol{\sigma}' : \mathbf{M} : \boldsymbol{\sigma}'} \tag{7}$$

where $\mathbf{M}$ stands for the Hill'48 orthotropic matrix representing the initial anisotropy of the metal sheet. With respect to the orthotropic coordinate system, the components of this matrix can be expressed in terms of Lankford's coefficients r_0, r_{45}, and r_{90}, leading to the following expression of the flow direction:

$$\mathbf{V} = \frac{\mathbf{M} : \boldsymbol{\sigma}'}{\overline{\sigma}} \tag{8}$$

The von Mises isotropic yield function can be seen as a particular case of the Hill'48 anisotropic yield function, from which it can be recovered for a particular value of $\mathbf{M}$.

In Eq. (4), the size of the current yield surface is given by the following:

$$Y = Y_0 + R \tag{9}$$

where Y_0 is the initial yield stress and R is the isotropic hardening variable. This variable is used to represent the evolution of the size of the yield surface and is physically related to the density of randomly distributed dislocations. Various macroscopic laws can be used to describe its evolution. For materials exhibiting hardening with a saturation level, Voce's law can be used:

$$\dot{R}_V = C_R (R_{\text{sat}} - R_V) \dot{\lambda} \tag{10}$$

where C_R and R_{sat} are material parameters that can be identified using classical monotonic tests. They represent the saturation rate and the saturation value of R_V, respectively. In the case of materials that do not exhibit any saturation of the hardening, Swift's power law is often used instead:

$$\dot{R}_S = nk\left(\frac{R_S + Y_0}{k}\right)^{\frac{n-1}{n}}\dot{\lambda} \tag{11}$$

where n and k are material parameters related to the growth rate of the yield surface, and $Y_0 = k\varepsilon_0^n$ is the initial yield stress providing the initial size of this surface. An equivalent, more classical form of this law can be written as shown below:

$$Y_S = k\left(\varepsilon_0 + \overline{\varepsilon}\right)^n = Y_0 + R_S \tag{12}$$

where $\overline{\varepsilon}$ denotes the equivalent plastic strain. Hollomon's law, which is used here for the analytical development of criteria based on the Maximum Force Principle, is a particular case of the Swift isotropic hardening law with an initial yield stress equal to zero, i.e., with no threshold for plastic yielding:

$$Y_H = k\overline{\varepsilon}^n = R_H \tag{13}$$

which can be rewritten in an equivalent form, with $Y_0 = 0$, as shown below:

$$\dot{R}_H = nk\left(\frac{R_H}{k}\right)^{\frac{n-1}{n}}\dot{\lambda} \tag{14}$$

All of these isotropic hardening laws can be expressed as the generic form shown below:

$$\dot{R} = H_R\dot{\lambda} \tag{15}$$

where H_R is the scalar isotropic hardening modulus, which can be found from Eqs. (10), (11), or (14), depending on the selected law. Using the previous equations and the consistency condition, it is possible to derive the relation between the stress and strain rates:

$$\dot{\boldsymbol{\sigma}} = \mathbf{L} : \mathbf{D} = \left(\mathbf{C} - \alpha^{ep}\frac{(\mathbf{C} : \mathbf{V}) \otimes (\mathbf{V} : \mathbf{C})}{\mathbf{V} : \mathbf{C} : \mathbf{V} + H_R}\right) : \mathbf{D} \tag{16}$$

where $\mathbf{L}$ and α^{ep} are the analytical elastic–plastic tangent modulus and a plastic loading flag equal to 1 during plastic loading and 0 in any other case, respectively. This general formulation allows for the modeling of a large class of materials. This description can be expanded by including damage effects.

2.2 Elastic–plastic model coupled with damage

Within phenomenological associative elastic–plastic modeling with a smooth yield surface, some material instability criteria, e.g., Rice's criterion, require a softening regime for the detection of localization. These softening effects can be obtained by coupling the constitutive equations with damage. Various damage approaches have been developed during the previous decades. Gurson's model [26–28] is one possible approach to describe the damage of elastic–plastic porous ductile media. Continuum damage mechanics is another approach that is based on the thermodynamics of irreversible processes [29, 30]. In this model, the damage variable is related to the surface density of micro-defects, such as voids, cavities or micro-cracks, on the surface of a representative elementary volume. This variable can be a second- or fourth-order tensor in the case of anisotropic damage, or a scalar in the case of isotropic damage. In this work, the softening effect is introduced by coupling the previous constitutive equations with isotropic damage. This coupling is carried out using the approach developed by Lemaitre [31], who introduced a scalar internal variable d related to the surface micro-defects. This variable is defined as the ratio of the surface of the defects S_{def} to the total surface S across a representative elementary volume of the material

$$d = \frac{S_{def}}{S} \tag{17}$$

and leads to the concept of the effective stress tensor shown below:

$$\boldsymbol{\sigma}_{eff} = \frac{\boldsymbol{\sigma}}{1-d} \tag{18}$$

By adopting the strain equivalence principle, the strain behavior of a damaged material is modeled using the constitutive laws of the undamaged material for which the usual stress is replaced by the effective stress [32]. The linear elasticity law can be written in its incremental form, leading to:

$$\dot{\boldsymbol{\sigma}} = (1-d)\mathbf{C} : (\mathbf{D} - \mathbf{D}^p) - \frac{\dot{d}}{1-d}\boldsymbol{\sigma} \tag{19}$$

where the plastic strain rate $\mathbf{D}^p$ can be expressed using the associative flow rule which verifies the normality relationship.

$$\mathbf{D}^p = \dot{\lambda}\frac{\partial F}{\partial \boldsymbol{\sigma}} = \dot{\lambda}\mathbf{V}_d \tag{20}$$

The yield criterion can be expressed as

$$\begin{aligned} &F = \overline{\sigma}\left(\boldsymbol{\sigma}'_{eff}\right) - Y \leq 0 \\ &\dot{\lambda} \geq 0 \\ &\dot{\lambda}F = 0 \end{aligned} \tag{21}$$

If the Hill'48 yield function is used, the plastic strain rate reads

$$\mathbf{D}^p = \frac{\dot{\lambda}}{(1-d)} \frac{\mathbf{M} : \boldsymbol{\sigma}'_{eff}}{\sqrt{\boldsymbol{\sigma}'_{eff} : \mathbf{M} : \boldsymbol{\sigma}'_{eff}}} \tag{22}$$

The stress variable does not enter explicitly the expressions of the isotropic hardening evolution laws discussed in the previous section; consequently, Eqs. (9)–(15) are still valid, and isotropic hardening can be written in the general form of Eq. (15).

The evolution of the ductile isotropic damage is related to the evolution of the microstructure of the material and in particular to the equivalent plastic strain rate $\dot{\bar{\varepsilon}}$. Lemaitre's ductile damage law links the evolution of the damage variable to the equivalent plastic strain rate and to the strain energy density release rate Y_e [33]. For linear isotropic elasticity, the strain energy density release rate Y_e can simply be written as

$$Y_e = \frac{J_2^2}{2E}\left[\frac{1}{2}(1+\nu) + 3(1-2\nu)\left(\frac{\sigma_{eff}^S}{J_2}\right)^2\right] \tag{23}$$

where $J_2(\boldsymbol{\sigma}_{eff}) = \sqrt{{}^3/_2 \boldsymbol{\sigma}'_{eff} : \boldsymbol{\sigma}'_{eff}}$ is the second invariant of the effective stress deviator, $\sigma_{eff}^S = {}^1/_3 tr(\boldsymbol{\sigma}_{eff})$ is the hydrostatic effective stress, E is the Young modulus and ν is the Poisson ratio of the undamaged material.

Improvements to Lemaitre's law have been proposed and recently applied to damage predictions during deep drawing simulation. These concern the introduction of an initial elastic energy threshold Y_{ei}, after which damage may occur, and the introduction of a material parameter β_d, governing the evolution of the damage variable:

$$\dot{d} = H_d \dot{\lambda} = \begin{cases} \dfrac{1}{(1-d)^{\beta_d}} \left(\dfrac{Y_e - Y_{ei}}{S_d}\right)^{s_d} \dot{\lambda} & \text{if } Y_e \geq Y_{ei} \\ 0 & \text{otherwise} \end{cases} \tag{24}$$

where S_d, s_d, and β_d are material parameters. By combining the consistency condition with Eqs. (19)–(24), the expression of the elastic–plastic tangent modulus coupled with damage $\mathbf{L}_d$ can be derived:

$$\dot{\boldsymbol{\sigma}} = \mathbf{L}_d : \mathbf{D} = \left((1-d)\mathbf{C} - \alpha^{ep} \frac{(1-d)^2 (\mathbf{C} : \mathbf{V}_d) \otimes (\mathbf{V}_d : \mathbf{C}) + H_d \boldsymbol{\sigma} \otimes (\mathbf{V}_d : \mathbf{C})}{(1-d)\mathbf{V}_d : \mathbf{C} : \mathbf{V}_d + H_R}\right) : \mathbf{D} \tag{25}$$

Further details on this derivation can be found in [34]. In the case of undamaged materials ($d=0$), the damage modulus H_d is null and $\mathbf{L}_d$ reduces to the undamaged expression $\mathbf{L}$ given in Eq. (16).

3 Popular sheet metal formability criteria

The aim of this section is to review the formability criteria most widely used to determine FLDs in the context of sheet metal forming. Within the Maximum Force Criteria, the onset of necking in the metal sheet is associated with a limit point that corresponds to a maximum of one or two particular load components applied to the material. Both diffuse and localized necking are predicted by criteria from this family [3–7]. Another successful family of models was initiated by Marciniak and Kuczyński [22]. In this family, an initial defect is considered to be in the sheet in the form of a band of reduced thickness, and localization is detected when the plastic strain is confined in this "groove" to a sufficient extent. Both approaches are still under active development. The majority of these developments are driven by applications and have led to numerous variants. Some of the most salient contributions are presented here in a unified manner, along with closed-form and numerical results.

Figure 1 illustrates the primary notations and conventions used in the following. Directions 1, 2, and 3 designate the principal directions of stress and strain rate. Direction 1 is the direction of the largest principal stress, whereas direction 3 designates the thickness direction. The plane-stress condition

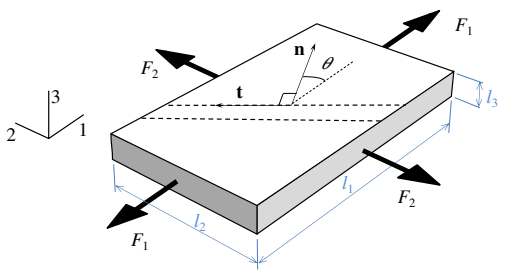

Fig. 1 Biaxial stretching of sheet material; notations

(σ_3=0) is assumed for all the models in this section. The stress and strain ratios

$$\alpha = \frac{\sigma_2}{\sigma_1}; \beta = \frac{\dot{\varepsilon}_2}{\dot{\varepsilon}_1} \tag{26}$$

are used to define the loading path, which is frequently considered linear (constant stress/strain-rate ratio). When localized necking is modeled, the neck is considered as a straight material band in the plane of the sheet along direction **t**; the normal **n** to the localized band lies in the plane of the sheet at an angle θ with respect to direction 1.

3.1 Maximum Force Criteria

This family of models includes the Considère and Swift criteria of diffuse necking, and the Hill'52 and Hora criteria of localized necking.

3.1.1 Considère criterion

The starting point of this approach is Considère's analysis of the uniaxial tension of metal bars. Considère [3] observed that diffuse necking for this configuration corresponds to the maximum applied load:

$$dF_1 = 0, \quad \text{with} \quad F_1 = \sigma_1 l_2 l_3 \tag{27}$$

By assuming incompressibility: $d\varepsilon_1+d\varepsilon_2+d\varepsilon_3=0$ (rigid plastic material), and differentiating Eq. (27), one obtains the well-known expression of Considère's criterion for diffuse necking under uniaxial tension

$$\frac{d\sigma_1}{d\varepsilon_1} = \sigma_1 \tag{28}$$

where ε_1 denotes the strain component in the tensile direction.

Most of the authors who have contributed to this class of models have provided the critical value of the sub-tangent Z defined in Fig. 2. It is noteworthy that this representation is restricted to the hypothesis of isotropic hardening, with the equivalent plastic strain $\bar{\varepsilon}$ being the only internal variable. Considering monotonic uniaxial tension, $Y \equiv \bar{\sigma} = \sigma_1$ and $\bar{\varepsilon} \equiv \varepsilon_1$, Eq. (28) leads to $\frac{1}{Z} = \frac{1}{Y}\frac{dY}{d\bar{\varepsilon}} = 1$.

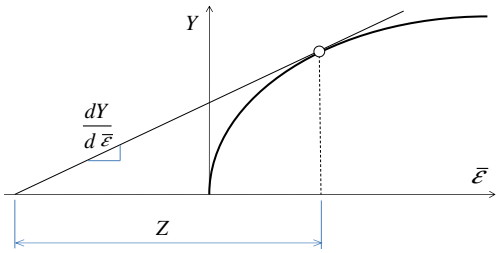

Fig. 2 The definition of the sub-tangent Z in the plot of the flow stress Y versus the equivalent plastic strain $\bar{\varepsilon}$

The maximum force approach has been extended to the two-dimensional loading case by Swift for diffuse necking [4], and by Hill and Hora et al. for localized necking [5, 6]. These developments are also based on the hypotheses of rigid plasticity and isotropic hardening, along with the more realistic plane-stress condition.

3.1.2 Swift criterion

Swift [4] extended the maximum load criterion to the case of biaxial loading by assuming that diffuse necking corresponds to the simultaneous maximum of the two components of the load: dF_1=0, dF_2 =0. Following the same approach as for Considère's criterion, one obtains

$$\frac{d\sigma_1}{d\varepsilon_1} = \sigma_1 \quad \text{and} \quad \frac{d\sigma_2}{d\varepsilon_2} = \sigma_2 \tag{29}$$

Differentiating the yield function for plane-stress conditions combined with Eq. (29), and substituting $d\varepsilon_1$ and $d\varepsilon_2$ with their expressions derived from the flow rule, one obtains a first expression for the derivative $d\bar{\sigma}/d\bar{\varepsilon}$. Then, combining the principle of equivalent work with the flow rule and rigid plasticity, one obtains a second expression for the equivalent stress $\bar{\sigma}$. The ratio of these two expressions gives a general form of the Swift'52 diffuse necking criterion, which is commonly known as the "Maximum Force Criterion" (MFC):

$$\frac{d\bar{\sigma}}{\bar{\sigma} d\bar{\varepsilon}} = \frac{\left(\frac{\partial\bar{\sigma}}{\partial\sigma_1}\right)^2 \sigma_1 + \left(\frac{\partial\bar{\sigma}}{\partial\sigma_2}\right)^2 \sigma_2}{\frac{\partial\bar{\sigma}}{\partial\sigma_1}\sigma_1 + \frac{\partial\bar{\sigma}}{\partial\sigma_2}\sigma_2} \tag{30}$$

A major criticism to the Swift'52 criterion is that, in the general case, special conditions that depend on the loading path or anisotropy are required to obtain simultaneous stationary loads [35]. Swift's hypothesis (29), on which the MFC is based, is rarely observed experimentally.

3.1.3 Hill'52 criterion

Hill's criterion [5, 36] is also based on a maximum force condition; however, it is specifically formulated to predict localized necking. This criterion is based on two statements: one that concerns the orientation of the localization band and a second that concerns the localization condition.

The first statement defines the orientation of the potential localization band along the instantaneous extensionless

direction in the plane of the sheet: $d\varepsilon_{tt}=0$. The angle θ defining this particular orientation in the principal stress frame is derived as

$$\theta = \arctan\sqrt{-\beta} \tag{31}$$

Classical particular cases concern simple shear ($\theta=45°$), uniaxial tension ($\theta=35°$), and plane strain tension ($\theta=0°$). Because no stationary extension exists in the domain of positive minor strains, the application of Hill's criterion is restricted to the left-hand side of the FLD.

The second statement defines the localization condition as the extremum of the load F_n normal to the localization band: $dF_n=0$. This leads, using the rigid plasticity assumption, to an expression similar in form to Considère's criterion: $d\sigma_n/d\varepsilon_n=\sigma_n$.

A more classical expression provides the critical subtangent in terms of the principal stresses, with the von Mises yield surface hypothesis:

$$\frac{1}{Y}\frac{dY}{d\overline{\varepsilon}} = \frac{\partial\overline{\sigma}}{\partial\sigma_1} + \frac{\partial\overline{\sigma}}{\partial\sigma_2} \tag{32}$$

The combination of the Hill'52 criterion for negative minor strains and the Swift'52 criterion for positive minor strains provided a simple and useful first approximation for the forming limit diagram prediction. However, the Swift'52 criterion was meant for diffuse necking and consistently underestimates the experimental FLDs. Also, its basic assumption of simultaneous maxima of the two load components is questionable. On one hand, this has been shown to never occur in proportional loading, which is typical for FLD determination. On the other hand, experimental observations suggest that during biaxial loading diffuse necking is related to the maximum of the load component which occurs first [37, 38]. Thus, modeling attempts have been made to predict localization on the right-hand side of the FLD by modifying Considère's original criterion [39]. The most successful attempt is attributed to Hora and coworkers and is known as the Modified Maximum Force Criterion (MMFC).

3.1.4 Hora criterion

This criterion [6] aims to predict localized necking on both sides of the FLD. It is an extension of Considère's formula (28) to the biaxial stress states, where the major principal stress σ_1 is considered to be a function of ε_1 and the strain-path parameter β: $\sigma_1=\sigma_1(\varepsilon_1,\beta)$.

In this biaxial loading context, Eq. (28) becomes the equation shown below, known as the Modified Maximum Force Criterion, which was later coined MMFC or Hora'06.

$$\frac{d\sigma_1}{d\varepsilon_1} = \frac{\partial\sigma_1}{\partial\varepsilon_1} + \frac{\partial\sigma_1}{\partial\beta}\frac{\partial\beta}{\partial\varepsilon_1} = \sigma_1 \tag{33}$$

The derivatives involved above can be further developed in terms of the equivalent stress and strain. Then, using the assumptions of plane stress, isotropic hardening, rigid plasticity, and proportional loading, one can write

$$\sigma_1 = f(\alpha)\overline{\sigma}\ ;\ \overline{\varepsilon} = g(\beta)\varepsilon_1\ ;\ \beta=\beta(\alpha) \tag{34}$$

and the derivatives

$$\frac{\partial\sigma_1}{\partial\overline{\sigma}} = f\ ;\ \frac{\partial\overline{\varepsilon}}{\partial\varepsilon_1} = g\ ;\ \frac{\partial\sigma_1}{\partial\beta} = \frac{\partial f}{\partial\alpha}\frac{\partial\alpha}{\partial\beta}\overline{\sigma} \tag{35}$$

where functions f and g depend on the expression of the yield surface. Using the yield condition $\overline{\sigma}=Y$, Eq. (33) becomes

$$\frac{1}{Y}\frac{\partial Y}{\partial\overline{\varepsilon}} = \frac{1}{fg}\left(f - \frac{\partial f/\partial\alpha}{\partial\beta/\partial\alpha}\frac{\partial\beta}{\partial\varepsilon_1}\right) \tag{36}$$

Finally, the proportional loading condition implies that

$$\beta = \frac{\varepsilon_2}{\varepsilon_1} \quad \text{and} \quad \frac{\partial\beta}{\partial\varepsilon_1} = -\frac{\varepsilon_2}{\varepsilon_1^2} = -\frac{\beta}{\varepsilon_1} \tag{37}$$

which completes the expression of the localization criterion in the well-established form

$$\frac{1}{Y}\frac{\partial Y}{\partial\overline{\varepsilon}} = \frac{1}{g} + \frac{\partial f/\partial\alpha}{f}\frac{\beta}{\partial\beta/\partial\alpha}\frac{1}{\overline{\varepsilon}} \tag{38}$$

A limitation of the Hora'96 Modified Maximum Force Criterion comes from the fact that it is not defined if $d\beta/d\alpha$ is null. In the case of materials modeled with the quadratic yield loci discussed in this paper, the MMFC remains applicable. However, Aretz [40] demonstrated that the MMFC can lead to a singularity when used with materials modeled using yield criteria exhibiting plane facets.

An additional modeling attempt was made by Mattiasson et al. [7] that takes into account an evolution of the strain path towards the plane strain after diffuse necking. The initially

constant strain path β_0 is used until diffuse necking is detected with a simplified Swift'52 criterion. Then, a variation of β is sought in order to verify Eq. (28) at each increment. The analysis is stopped when the strain path is close to plane strain, which is determined by a comparison of the current strain path with a user-defined threshold. It should be noted that for the resulting criterion, the Enhanced Maximum Force Criterion, according to the authors, the FLD is constructed by plotting the minor limit strain ε_2 and its pair along the initial strain path β_0, i.e., $(\varepsilon_2/\beta_0, \varepsilon_2)$. Consequently, the limit points appear on the original (linear) strain path and can be conveniently compared to other models with these assumptions.

3.1.5 FLD predictions of the Maximum Force Criteria

The strength of the maximum force approach is that it leads to simple mathematical expressions, allowing closed-form analytical solutions in many cases. The expression of the subtangent Z depends on the choice of the yield surface, whereas the limit strains depend on the hardening model. In order to analytically compare the different criteria, the simple von Mises yield surface (5) (restricted to isotropic hardening and plane stress) and the Hollomon hardening law (13) were chosen. In this case, the relationship between α and β becomes

$$\alpha = \frac{2\beta + 1}{\beta + 2} \;\; ; \;\; \beta = \frac{2\alpha - 1}{2 - \alpha} \tag{39}$$

For Hora's criterion, the functions f and g are written as shown below:

$$f = \frac{1}{\sqrt{1 - \alpha + \alpha^2}} \;\; ; \;\; g = \frac{2}{\sqrt{3}} \sqrt{1 + \beta + \beta^2} \tag{40}$$

After differentiation, these expressions are included in the respective formulas of Z and of the major limit strain ε_1 previously derived for the four criteria: Considère, Swift, Hill, and Hora. The resulting closed-form expressions are summarized in Table 1, as functions of the strain-path parameter β. Numerical values are also provided for four specific values of β that correspond to simple shear ($\beta = -1$), uniaxial tension ($\beta = -1/2$), plane strain tension ($\beta = 0$), and balanced biaxial tension ($\beta = 1$). All of the predictions coincide remarkably for plane strain ($\varepsilon_1 = n$), which indicates that diffuse and localized necking tend to each other for this particular straining mode. For uniaxial tension, the diffuse necking predictions of Considère and Swift'52 (identical) occur significantly earlier than the localized necking predictions of Hill'52 and Hora. The latter predictions differ for $n \neq 1/3$. The same trend is observed for expansion, with Swift's criterion activated prior to Hora's. However, the simple shear yields inconsistent results: Hora'96 is the only criterion that predicts localization for this straining mode, whereas Swift'52 and Hill'52 predict stable flow for any strain level.

The limit strain analytical expressions from Table 1 were used to plot the FLDs shown in Fig. 3 for the particular case of $n = 0.18$. These predictions are compared qualitatively to the experimental FLDs determined by Banabic et al. [41] for an aluminum alloy. Swift's criterion indicates diffuse necking, thus exhibiting very conservative predictions. Hill'52 criterion shows a very good correlation for the left-hand side of the FLD, while Hora's criterion describes well the right-hand side of the FLD. It is noteworthy that the experimental results do not exhibit a distinct forming limit "curve"; the limit between safe and failed experimental strain points is a zone with a non-negligible width, which makes the validation of the models a delicate task. It is however remarkable that these closed-form analytical criteria are capable of capturing the most salient features of the experimental FLDs using such very simple material modeling and no fitting parameters.

For a quantitative comparison to experimental FLDs, more complex constitutive models (anisotropic yield surface, or different isotropic hardening model) should be used. In this case, analytical expressions are difficult to obtain; therefore, numerical predictions are required. Figure 4 shows the influence of the hardening and anisotropy parameters, for the case of Hill's 1948 quadratic yield criterion combined with Swift's hardening law. The default material parameters used in these simulations are summarized in Table 2. The expected influence of these material parameters was predicted, particularly the significant sensitivity of the FLD to the hardening coefficient. The predictions of the Hill'52 localization criterion were not affected by anisotropy[1], and its influence was negligible in the case of the Swift'52 criterion. This may explain the lasting footprint left by the analytical Hill–Swift FLD in this research field. For all of the maximum force criteria shown in Fig. 4, the forming limit in plane strain was insensitive to anisotropy, and the r_{45} anisotropy coefficient had no influence on the forming limit diagrams. The r_0 and r_{90} coefficients primarily affected the predictions given by Hora's criterion. The increase of r_0 lowered both sides of the FLD, whereas r_{90} mainly affected the left side (increase)[2].

[1] This does not mean that with this model, the beneficial influence of anisotropy on formability is not predicted, e.g., in the case of uniaxial tension: for a larger r value, the tensile strain path moves leftwards and thus the limit strains do increase, even if the FLD does not change.

[2] The major strains are applied in the rolling direction, throughout the paper.

Table 1 The analytical predictions of the maximum force criteria for the von Mises and Hollomon laws; the minor limit strain is $\varepsilon_2=\beta\varepsilon_1$

Criterion	$\frac{1}{Z}$	Major limit strain ε_1				
		Equation	Numerical values			
			$\beta=-1$	$\beta=-1/2$	$\beta=0$	$\beta=1$
Considère	1	n	–	n	–	–
Swift	$\frac{\sqrt{3}}{2}\frac{B}{A}\frac{1+\beta}{\sqrt{A}}$	$\frac{A}{B}\frac{1}{1+\beta}n$	∞	n	n	n
Hill'52	$\frac{\sqrt{3}1+\beta}{2\sqrt{A}}$	$\frac{1}{1+\beta}n$	∞	$2n$	n	–
Hora	$\frac{\sqrt{3}}{2}\frac{1}{\sqrt{A}}-\frac{3\beta^2}{2A(2+\beta)}\frac{1}{g\varepsilon_1}$	$n+\frac{3\beta^2}{2(2+\beta)A}$	$n+3/2$	$n+1/3$	n	$n+1/6$

$A=1+\beta+\beta^2$ and $B=1-\frac{1}{2}\beta+\beta^2$.

3.2 Marciniak–Kuczyński (M–K) model

The Marciniak–Kuczyński model (M–K) is based on the semi-empirical observation stating that necking occurs at an initial imperfection of the structure [22]. For this criterion, heterogeneity with degraded properties is initially introduced into the sheet metal. This defect can be introduced under a geometrical or material form; however, it is often reproduced in the structure as a band of reduced thickness. In the original M–K model, the normal **n** to this band was fixed and oriented along direction 1. In the following equations, the superscript "B" designates the physical quantities in the band. The initial defect f_0 is defined as $f_0=t_0^B/t_0$, where t_0 is the initial thickness. The value of the initial defect is generally assumed to be between 0.99 and 1. A significant drawback to this approach is that the postulated initial imperfection has an important influence on the FLD, while it does not carry significant physical meaning. However, it can be viewed as an equivalent heterogeneity.

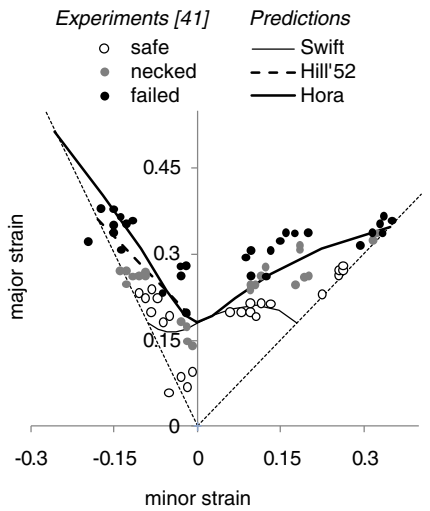

Fig. 3 The forming limit diagrams predicted by the maximum force criteria for a von Mises material obeying Hollomon's hardening law with $n=0.18$, and qualitative comparison to the experimental FLDs taken from [41]

The basis of the M–K analysis is to compare the evolution of the mechanical or geometrical properties inside and outside of the band. Plane stress and planar anisotropy are assumed. The computation of the mechanical states in the two areas is performed separately. During loading, the components of the stress and/or strain rate tensors are imposed in the safe area, and the mechanical state is computed from the constitutive equations. The following equilibrium and compatibility equations and the evolution of the defect f are then used to compute the mechanical state inside the band:

$$\begin{cases} \sigma_{nn}^B t^B = \sigma_{nn} t \\ \sigma_{nt}^B t^B = \sigma_{nt} t \\ \dot{\varepsilon}_{tt}{}^B = \dot{\varepsilon}_{tt} \\ f = f_0 \exp\left(\varepsilon_{33}^B - \varepsilon_{33}\right) \end{cases} \tag{41}$$

where **n** and **t** denote the normal and the tangential direction to the band, respectively, whereas t and t^B are the current thicknesses of the sheet and of the band, respectively. From these equations, it is possible to determine the mechanical state inside the band.

Mechanical or geometrical properties of the safe area and of the defect zone are then compared to detect localization. The choice of these mechanical properties has a clear influence on the predicted FLD. It is common to use the ratio of major principal strain rates, but it is possible to use the ratio of strain rates in the thickness direction or the ratio of equivalent strain rates: $\bar{\dot{\varepsilon}}^B/\bar{\dot{\varepsilon}} > S_{M-K}$, where S_{M-K} is the threshold of the criterion (i.e., the critical value). When the latter inequality is satisfied, localization is predicted.

Hutchinson and Neale observed that the original formulation of the criterion overestimates the FLD predictions on the left side of the curve [42]. In this zone of negative minor strains, it is known (from experiments and from the Hill'52

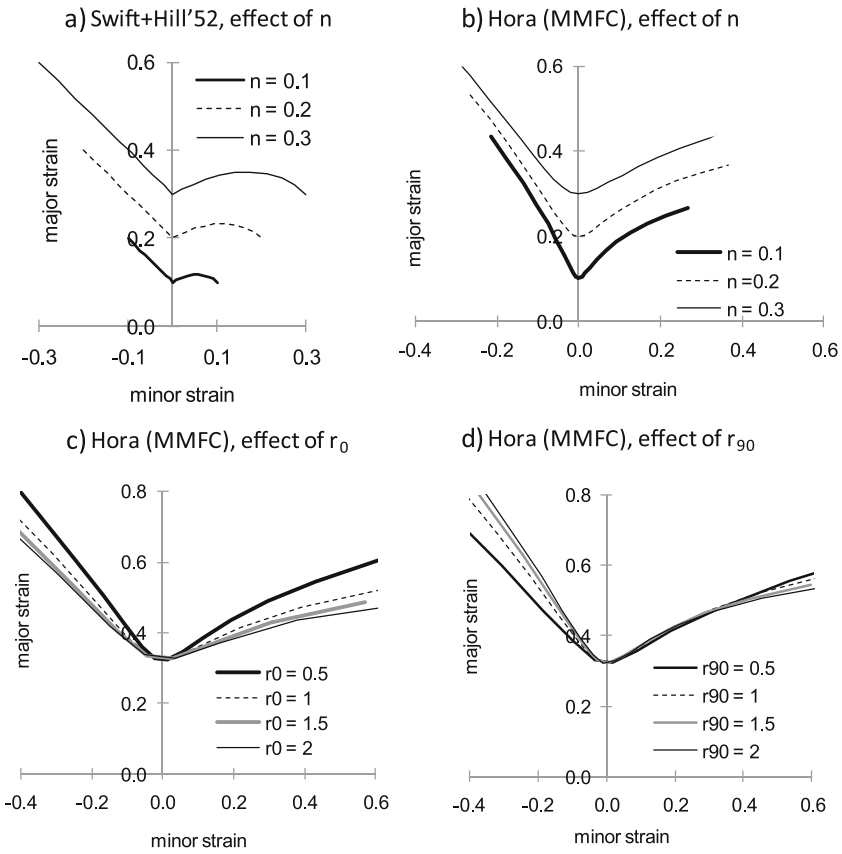

Fig. 4 The influence of the hardening parameter n and the anisotropy coefficients r_0 and r_{90} on the forming limit diagrams predicted by the maximum force criteria (**a** Swift'52 and Hill'52; **b**–**d** Hora). The Hill'48 quadratic yield function and Swift's hardening law were used; the default values of the material parameters are provided in Table 2

predictions) that the localization band is no longer perpendicular to the largest principal stress axis. Accordingly, Hutchinson and Neale [42] extended the M–K analysis to arbitrary orientations θ of the band. The evolution of the orientation angle during the analysis is updated with the formula:

$$\tan(\theta) = e^{(1-\beta)\varepsilon_{11}} \tan(\theta_0) \tag{42}$$

In the expansion part of the FLDs (right-hand side), the effect of the initial orientation θ_0 of the band is more limited, and it is generally not necessary to test all of the initial orientations of the band to minimize the FLD. It is noteworthy that the M–K model provides a useful complement to the Hill'52 criterion for the predictions of strain localization, and these two models are still used in recent publications due to their simplicity and effectiveness (e.g., [40]).

The M–K analysis is based on the comparison of the evolution of mechanical fields, for example the equivalent strain rates, in both the safe and defective areas of the metal sheet. The constitutive laws do not appear explicitly in the localization criterion, making it easy to couple this criterion with advanced phenomenological or micromechanical material modeling and to include the effects of microstructure, damage or strain rate sensitivity.

Table 2 Material parameters used as reference for the predictions in Fig. 4 [41]

k [MPa]	n	ε_0	r_0	r_{45}	r_{90}
585.2	0.3232	0.004926	0.642	1.039	0.829

The FLDs predicted with the M–K model differ from those of the maximum force criteria. Figure 5 compares their predictions for a brass material whose parameters are reported in Table 3. While the Maximum Force Criteria agree for plane strain tension predictions, the overall predictions of Hora's criterion are delayed compared to the Swift'52 or the Hill'52 predictions. It is noteworthy that Hora's FLD is not strictly higher than the Swift'52 one because their values are identical in plane strain whereas their slopes are not. This illustrates the fact that the Hora'96 criterion is an extension of Considère's criterion, not Swift's criterion as sometimes stated. The M–K analysis predicts lower limit strains for plane strain tension, while for uniaxial and balanced biaxial tension, it overpredicts Hora's FLD. Modifying the user-defined parameters of the M–K method will reduce one or the other of these differences, but not both, because the entire FLD will be shifted by this operation.

Since they predict distinct shapes of the FLD, all of these criteria are equally applied in the literature to various metal sheets [8, 9, 43, 44]. Indeed, even within the same family of

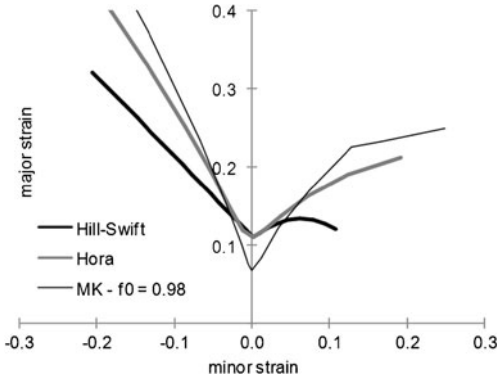

Fig. 5 The forming limit diagrams predicted with criteria based on the Maximum Force principle and the M–K theory and the material parameters from Table 3

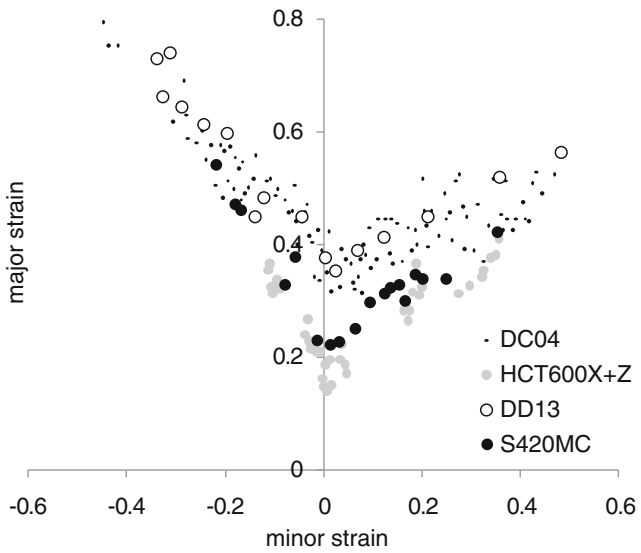

Fig. 6 Experimental FLDs determined by Abspoel et al. [45] for several sheet steel grades

sheet metals, the shape of the FLD can vary from grade to grade and these differences do not generally reduce to a simple scaling factor. This is illustrated by the experimental FLDs of several steel grades shown in Fig. 6, taken from reference [45]. It appears from the figure that the two mild steels (hot and cold rolled) have very similar FLDs; Hora's criterion seems to be well suited to describe their shape. For higher grade steels, the limit strains are decreasing, but they do so more in the plane strain region than in uniaxial tension and balanced biaxial expansion. Consequently, the M–K model may be successful to describe the formability of some of these sheet steels, with a suitable fitting of its initial defect parameter.

In terms of compatibility with more advanced constitutive models, the Maximum Force Criteria, although computationally very efficient, have their theoretical formulations restricted to isotropic hardening, rigid plasticity, and linear strain paths. The more laborious M–K model allows for a wider range of materials and constitutive models, while making use of a user-defined (non-physical) parameter.

Another approach to predict material instability in sheet metals is provided by the bifurcation analysis. With a theoretically sound background, this approach is systematically used to predict localization, e.g., in geomechanics; however, it is seldom applied to formability predictions in sheet metal forming. This is discussed in the next section.

4 Bifurcation analysis

The occurrence of diffuse necking can be regarded as a gradual evolution from a homogeneous deformation state to a heterogeneous one. However, strain localization can be seen as a more rapid transformation from a quasi homogeneous deformation mode to a localized discontinuous mode. Following this approach, a bifurcation analysis can be used to predict necking and localization phenomena.

Table 3 The material parameters of a brass material [20]

k (MPa)	n	ε_0	r_0	r_{45}	r_{90}
618.3	0.118	0.014	1.8	1.3	2.0

4.1 The General Bifurcation and the Limit-Point Bifurcation criteria

Drucker [46] and then Hill [11] introduced a necessary condition for the loss of uniqueness of the solution of the boundary value problem for rate independent materials. The starting point for this approach is the variational principle governing the equilibrium equations for any kinematically admissible virtual velocity field (i.e., satisfying the boundary conditions). By considering two different solutions for the associated boundary value problem, a sufficient condition for uniqueness is obtained by the positiveness of the second-order work, as follows:

$$\dot{\mathbf{F}} : \mathbf{K}_d : \dot{\mathbf{F}} > 0 \tag{43}$$

where $\mathbf{K}_d$ is the tangent modulus relating the first Piola–Kirchhoff stress rate tensor $\dot{\mathbf{\Pi}}$ to the velocity gradient $\dot{\mathbf{F}}$, as: $\dot{\mathbf{\Pi}} = \mathbf{K}_d : \dot{\mathbf{F}}$, which, within an updated Lagrangian approach, reads

$$K_{d\ ijkl} = L_{d\ jikl} + \sigma_{ji}\delta_{kl} - \frac{1}{2}\left(\sigma_{li}\delta_{jk} + \sigma_{ki}\delta_{jl}\right) - \frac{1}{2}\left(\sigma_{jk}\delta_{il} - \sigma_{jl}\delta_{ik}\right) \tag{44}$$

where the components $L_{d\,jkl}$ are those of the tangent modulus $\mathbf{L}_d$ given in Eq. (25).

This sufficient condition for uniqueness is then given by the verification of the positive definiteness of the quadratic form of Eq. (43) and, in practice, by the verification that all of the eigenvalues of the symmetric part of $\mathbf{K}_d$ are positive. The corresponding General Bifurcation condition can be seen as a lower bound for diffuse or localized necking.

For a special case of the General Bifurcation condition, known as the Limit-Point Bifurcation [12], necking is associated with a stationary stress state: $\dot{\mathbf{\Pi}} = \mathbf{0}$, leading to

$$\mathbf{K}_d : \dot{\mathbf{F}} = \mathbf{0} \tag{45}$$

This criterion is then associated with the singularity of the tangent modulus $\mathbf{K}_d$, and the limit point is reached when its first eigenvalue reaches a value of zero. It predicts the loss of uniqueness of the solution of the equilibrium problem associated with a stationary stress state. In practice, the latter criterion is less conservative than the general bifurcation criterion.

For the case of small deformations and associative elasto-plasticity, the tangent modulus is symmetric. The General Bifurcation (i.e., violation of Eq. (43)) and Limit-Point Bifurcation (Eq. (45)) criteria lead then to the same results and can predict the occurrence of diffuse or localized necking. Other criteria have been developed to predict localized modes of necking.

4.2 The loss of ellipticity and the loss of strong ellipticity criteria

For the loss of ellipticity and the loss of strong ellipticity criteria, localization is viewed as an abrupt evolution of the velocity gradient from a homogeneous state to a heterogeneous state exhibiting discontinuity planes in the velocity gradient. Two discontinuity planes of normal $\mathbf{N}$ define a localization band (see Fig. 7). Localization corresponds to a bifurcation of the governing equations associated with a discontinuous compatible strain rate.

Denoting by $\dot{\mathbf{F}}^B$ and $\dot{\mathbf{F}}$, the velocity gradient inside and outside a possible localization band, respectively, the associated jump will be denoted: $[\dot{\mathbf{F}}] = \dot{\mathbf{F}} - \dot{\mathbf{F}}^B$. Such a discontinuity of the velocity gradient across the localization band leads to the existence of a non-zero vector $\dot{\mathbf{c}}$ that represents the relative velocities between the areas located at each side of the discontinuity planes, such that the Hadamard compatibility condition is satisfied [47]:

$$\dot{\mathbf{F}} = \dot{\mathbf{F}}^B + \dot{\mathbf{c}} \otimes \mathbf{N} \tag{46}$$

A second condition, the continuity of the force across the localization band planes, must be verified. Written in the rate form and with the first Piola–Kirchhoff stress tensor, this leads to

$$[\dot{\mathbf{\Pi}}] \cdot \mathbf{N} = \mathbf{0} \tag{47}$$

By introducing the nominal stress tensor $\mathcal{N}$ as the transpose of the first Piola–Kirchhoff stress tensor, the constitutive relation can be rewritten as: $\dot{\mathcal{N}} = \mathbf{T}_d : \dot{\mathbf{F}}$, where the tangent modulus $\mathbf{T}_d$ can be expressed in terms of $\mathbf{K}_d$, defined in Eq. (44), as $T_{d\,ijkl} = K_{d\,jkl}$.

Combining the above equations, a necessary condition for a non-trivial solution for vector $\dot{\mathbf{c}}$ is derived, which provides a localization criterion expressed as follows:

$$\det(\mathbf{N} \cdot \mathbf{T}_d \cdot \mathbf{N}) = 0 \tag{48}$$

In practice, the numerical prediction of localization is carried out by the search for the first value of the tangent modulus leading to a singularity of the acoustic tensor $\mathbf{N} \cdot \mathbf{T}_d \cdot \mathbf{N}$ during the loading of the metal sheet. For each loading increment, the determinant of the acoustic tensor is computed for all orientations of the normal to the band. For the first loading increment allowing singularity of the acoustic tensor, localization is predicted. The critical strains at localization, the orientation of the localization band, and the localization mode are given by the deformation at that loading increment, by the normal $\mathbf{N}$ and, if computed, by vector $\dot{\mathbf{c}}$, respectively. If $\mathbf{N}$ and $\dot{\mathbf{c}}$ are parallel or orthogonal, an opening mode or a shear mode, respectively, develops; otherwise, the mode is said to be combined.

Similar to the condition of loss of ellipticity (48), the condition for loss of strong ellipticity can be obtained as follows:

$$\dot{\mathbf{c}} \cdot (\mathbf{N} \cdot \mathbf{T}_d \cdot \mathbf{N}) \cdot \dot{\mathbf{c}} = 0 \tag{49}$$

This strong ellipticity condition implies the verification of the positive definiteness of the quadratic form $\dot{\mathbf{c}} \cdot (\mathbf{N} \cdot \mathbf{T}_d \cdot \mathbf{N}) \cdot \dot{\mathbf{c}}$, and therefore, the verification that all of the eigenvalues of the symmetric part of the acoustic tensor $(\mathbf{N} \cdot \mathbf{T}_d \cdot \mathbf{N})^s$ are positive [48, 49].

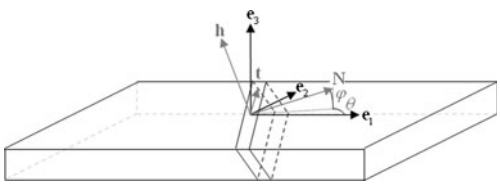

Fig. 7 The orientation of the localization band of normal $\mathbf{N}$ for the loss of ellipticity and the loss of strong ellipticity models

From the previous derivations, it is shown that the limit-point bifurcation and loss of strong ellipticity criteria are less conservative than the general bifurcation criterion, and that the loss of ellipticity criterion is less conservative than the loss of strong ellipticity criterion [49].

4.3 Application of the bifurcation analysis criteria to FLDs

For the criteria based on the bifurcation analysis, softening is required to detect strain localization; this effect is introduced by coupling the elastic–plastic model with damage. These criteria make no other hypothesis for the constitutive model, which can describe quite general rate-independent elastic–plastic behavior. For the current application, the Hill'48 quadratic yield function (7) is considered with an isotropic hardening model (9)–(10) and the isotropic continuum damage model presented in Section 2.2. The set of material parameters used for the simulations is summarized in Table 4 and the predicted FLDs are shown in Fig. 8.

The numerical results conform to the theoretical observations stating that the general bifurcation is the most conservative criterion in this series, while the loss of ellipticity occurs last. For the case of associative plasticity, because the tangent modulus that enters the expression of the acoustic tensor is almost symmetric, the four criteria are not all distinct. The limit point and general bifurcation criteria, which can be associated with the diffuse necking phenomenon, occur simultaneously. Similarly, the predictions of the loss of ellipticity and the loss of strong ellipticity criteria overlap; however, they appear later than the limit point and general bifurcation criteria as they predict strain localization. It is noteworthy that for the plane strain tension mode, diffuse and localized necking criteria tend to predict close limit strain values, as observed in Section 3.

As previously discussed, the use of more advanced behavior models, e.g., combined hardening or damage coupling, prevents the application of the maximum force criteria. However, the M–K analysis can still be applied in conjunction with the constitutive model selected in this section. Figure 9 shows the comparison of the strain localization predictions obtained with Rice's loss of ellipticity criterion and the M–K method. Although they belong to different criteria categories, the two types of predictions have common features. The damage affects mainly the expansion zone of the FLD, and the limit strains strongly diminish in the neighborhood of plane strain

Table 4 The material parameters of a Dual-Phase steel [34] modeled with the Hill'48 yield surface, isotropic hardening and isotropic damage

Y_0 [MPa]	R_{sat} [MPa]	C_R	r_0	r_{45}	r_{90}	β_d	S_d	s_d	Y_{ei}
356.1	551.4	9.3	1	1.5	2	5	20	0.01	0

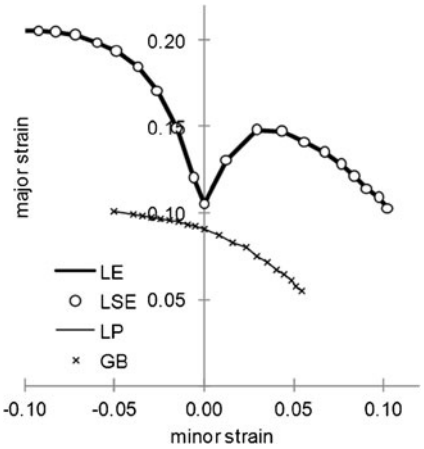

Fig. 8 The FLDs of a dual-phase steel obtained with criteria based on the bifurcation analysis. LE stands for loss of ellipticity, LSE for loss of strong ellipticity, LP for limit-point bifurcation, and GB for general bifurcation

tension. Also, the loss of ellipticity criterion appears to be an upper bound with respect to the M–K predictions. Note that this formal analogy between the M–K formulation and the bifurcation equations has already been noticed by Tvergaard [50], where the former has been shown to reduce to the Stören–Rice type bifurcation [15] when the initial imperfection is set to be zero. However, this formal comparison of the two approaches has been made in the context of the finite strain version of the J_2 deformation theory of plasticity, initially proposed by Stören and Rice [15], which introduces vertex effects on the current points of the yield surface. It is noteworthy that such yield surface vertices are known to be destabilizing effects that trigger localization bifurcation in the

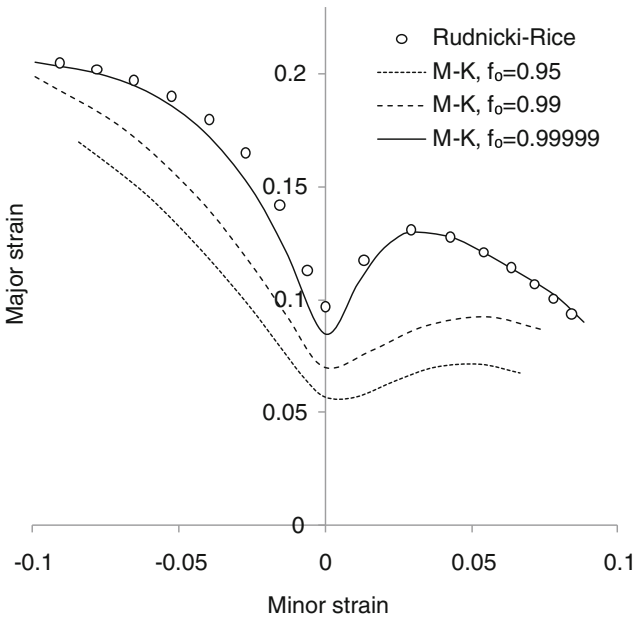

Fig. 9 The forming limit diagrams of a dual-phase steel obtained with the M–K criterion and with Rice's loss of ellipticity criterion

Table 5 Summary of the assumptions and interpretation of the investigated criteria

Criterion	Diffuse / Localized necking	Meaning / interpretation of the criterion	Hypotheses / applicability range				
			Plane stress, rigid-plasticity, isotropic hardening	Rate-independent behavior	Closed-form expression*	Requires fitting parameter	Other remarks
Considère	D	Maximum of the uniaxial tensile load	■		■		Uniaxial tensile loading only
Swift	D	Simultaneous maximum of major/minor load components	■		■		Assumes simultaneous load maxima
Hill'52	L	Maximum load normal to the instantaneous extensionless direction	■		■		Only for negative minor strains
Hora'96	L	Maximum of the major load component	■		■		Singularity issue for yield criteria with plane facets
M–K	L	Strain rate much larger in the defect zone				■	Assumes an initial defect zone + plane stress
General Bifurcation	D	Loss of uniqueness for the solution of the boundary value problem		■			
Limit-Point Bifurcation	D	Loss of uniqueness associated with a stationary stress state		■			
Loss of Strong Ellipticity	L	Loss of strong ellipticity for the equations of the boundary value problem		■			Need either softening (e.g., by coupling with damage) or vertex effects (deformation theory, crystal plasticity, non-normality…)
Loss of Ellipticity	L	Incipience of a plane band with discontinuity of velocity gradient		■			

* Closed-form expressions provided in the case of von Mises yield surface and Hollomon hardening law

positive hardening regime, without the need for introducing any softening mechanisms. In the current contribution, the comparison between the M–K imperfection approach and the bifurcation analysis is carried out in the context of a smooth yield surface and classical associative elasto-plasticity coupled with damage, in which the destabilizing mechanism is attributed to damage-induced softening. Similar observations and trends are revealed; in particular, the M–K

predictions tend towards the bifurcation results in the limit of vanishing size for the assumed initial imperfection, as can be seen in Fig. 9.

5 Summary and conclusions

A significant part of this contribution consisted in the effort made in providing, within a single document, the most recognized approaches for the prediction of diffuse and localized necking and the associated sheet forming limits. The first step in this attempt was to organize the selected criteria into three main classes, on the basis of their physical background and theoretical foundations. These three classes of instability criteria are based on the principles of maximum force, initial defect (M–K), and bifurcation. Then, the formulations of these various criteria were rewritten in a unified, general modeling framework, including large deformation anisotropic elasto-plasticity coupled with damage and isotropic hardening. Particular modeling restrictions (i.e., plane stress, rigid plasticity, isotropic hardening, or damage) were further applied to some criteria according to their respective hypotheses, which were systematically clarified. In the case of the bifurcation analysis, it was possible to theoretically establish a hierarchy between the limit strain values predicted by each criterion. Numerical predictions for materials selected from the literature allowed for the validation of these observations and for a wider comparison of the various criteria and models.

The respective strengths and weaknesses of the different criteria, with regard to generality, applicability range, modeling assumptions, have been clearly and systematically specified. For example, the very attractive closed-form expressions afforded by the maximum force criteria require, in turn, some strong theoretical restrictions (i.e., plane stress, rigid plasticity, isotropic hardening, etc.). Hora's criterion is the most widely used in this category; because Considère's criterion is restricted to uniaxial tension, Swift's criterion assumes simultaneous stationary loads, which is rarely observed experimentally, and Hill'52 approach is restricted to negative minor strains. The M–K imperfection approach is also widely used and its popularity lies in its compatibility with virtually any constitutive modeling. Its major drawback, however, is the strong dependence of its predictions on the arbitrarily postulated initial defect. As to bifurcation theory, although based on sound theoretical foundations, it is only applicable to rate-independent materials. Also, for strain localization predictions, the bifurcation theory requires softening, which can be introduced by coupling with damage, or vertex effects, as induced by the deformation theory or crystal plasticity. Table 5 hereafter summarizes the modeling assumptions, interpretation, and applicability range of the investigated criteria.

The simulations performed for some materials taken from the literature reveal that distinct FLDs are predicted, and the final result may depend more on the instability approach than on the constitutive model. Thus, it is likely that none of these criteria performs systematically better than the others in the general case. In practice, a criterion is mainly chosen for its compatibility with the constitutive model required for the simulation of the sheet metal forming. The majority of the criteria imply particular modeling restrictions, e.g., isotropic hardening, strain-rate independence, or damage. Nevertheless, theoretical and numerical similarities were emphasized between several criteria. In particular, the M–K and bifurcation analyses exhibited some common features, which result from the formal analogy in their governing equations. Finally, experimental validation must be performed on a large number of materials before general conclusions may be drawn concerning the most appropriate instability criteria for industrial application. Recasting these models into a common modeling context was completed as a prerequisite to a thorough validation.

Acknowledgments Part of this work has been funded by the French National Research Agency ANR under project 'FORMEF'. G. A. was financially supported by the Centre National de la Recherche Scientifique and the Région Lorraine.

References

1. Keeler SP (1965) Determination of forming limits in automotive stampings. Sheet Met Ind 42(461):683–691
2. Keeler SP, Backofen A (1963) Plastic instability and fracture in sheets stretched over rigid punches. Metall Trans A 56:25
3. Considère A (1885) Mémoire sur l'emploi du fer et de l'acier dans les constructions. Annales des Ponts et Chaussées 9:574
4. Swift HW (1952) Plastic instability under plane stress. J Mech Phys Solid 1(1):1–18
5. Hill R (1952) On discontinuous plastic states, with special reference to localized necking in thin sheets. J Mech Phys Solid 1(1):19–30
6. Hora P, Tong L, Reissner J (1996) A prediction method of ductile sheet metal failure in FE simulation. In: Numisheet 1996, Dearborn, Michigan, USA, pp 252–256
7. Mattiasson K, Sigvant M, Larson M (2006) Methods for forming limit prediction in ductile metal sheets. In: IDDRG 2006, Porto, Portugal, pp 1–9
8. Brunet M, Morestin F (2001) Experimental and analytical necking studies of anisotropic sheet metals. J Mater Process Technol 112: 214–226
9. Ben Tahar M (2005) Contribution à l'étude et la simulation du procédé d'hydroformage. PhD Thesis, ENSMP, Nice
10. Drucker DC (1956) On uniqueness in the theory of plasticity. Q Appl Math 14:35–42
11. Hill R (1958) A general theory of uniqueness and stability in elastic–plastic solids. J Mech Phys Solid 6(3):236–249
12. Valanis KC (1989) Banding and stability in plastic materials. Acta Mech 79(1–2):113–141
13. Rice JR (1976) The localization of plastic deformation. In: 14th International Congress on Theoretical and Applied Mechanics. North-Holland, Delft, Netherlands, pp 207–220

14. Rudnicki JW, Rice JR (1975) Conditions for the localization of deformation in pressure-sensitive dilatant materials. J Mech Phys Solid 23(6):371–394
15. Stören S, Rice JR (1975) Localized necking in thin sheets. J Mech Phys Solid 23(6):421–441
16. Asaro RJ, Rice JR (1977) Strain localization in ductile single crystals. J Mech Phys Solid 25(5):309–338
17. Franz G, Abed-Meraim F, Ben Zineb T, Lemoine X, Berveiller M (2009) Role of intragranular microstructure development in the macroscopic behavior of multiphase steels in the context of changing strain paths. Mater Sci Eng A 517(1–2):300–311
18. Franz G, Abed-Meraim F, Ben Zineb T, Lemoine X, Berveiller M (2013) Strain localization analysis for single crystals and polycrystals: towards microstructure-ductility linkage. Int J Plast 48: 1–33
19. Dudzinski D, Molinari A (1991) Perturbation analysis of thermoviscoplastic instabilities in biaxial loading. Int J Solids Struct 27(5):601–628
20. Lejeune A, Boudeau N, Gelin JC (2003) Influence of material and process parameters on bursting during hydroforming process. J Mater Process Technol 143–144(1):11–17
21. Benallal A (2000) Perturbation and stability of rate-dependent solids. Eur J Mech Solid 19(special issue):45–60
22. Marciniak Z, Kuczyński K (1967) Limit strains in the processes of stretch-forming sheet metal. Int J Mech Sci 9(9):613–620
23. Ghosh AK (1974) Strain localization in the diffuse neck in sheet metal. Metall Mater Trans B 5(7):1607–1616
24. Reyes A, Hopperstad OS, Berstad T, Lademo OG (2008) Prediction of necking for two aluminium alloys under non-proportional loading by using a FE-based approach. Int J Mater Form 1(4):211–232
25. Haddag B, Balan T, Abed-Meraim F (2007) Investigation of advanced strain-path dependent material models for sheet metal forming simulations. Int J Plast 23(6):951–979
26. Gurson AL (1977) Continuum theory of ductile rupture by void nucleation and growth: Part 1—yield criteria and flow rules for porous ductile media. J Eng Mater Technol Trans ASME 99(1):2–15
27. Needleman A, Rice JR (1978) Limits to ductility set by plastic flow localization. In: Koistinen DP, Wang NM (eds) Mechanics of sheet metal forming. Plenum, New York, pp 237–267
28. Tvergaard V, Needleman A (1984) Analysis of the cup–cone fracture in a round tensile bar. Acta Metall 32(1):157–169
29. Kachanov LM (1986) Introduction to continuum damage mechanics. Martinus Nijhoff, Dordrecht
30. Rabotnov YN (1969) Creeps problems in structural members. North-Holland, Amsterdam
31. Lemaitre J (1985) Continuous damage mechanics model for ductile fracture. J Eng Mater Technol Trans ASME 107(1):83–89
32. Lemaitre J, Chaboche JL (1990) Mechanics of solid materials. Cambridge University Press, Cambridge
33. Lemaitre J (1992) A course on damage mechanics. Springer, Berlin
34. Haddag B, Abed-Meraim F, Balan T (2009) Strain localization analysis using a large deformation anisotropic elastic–plastic model coupled with damage. Int J Plast 25(10):1970–1996
35. Habbad M (1994) Instabilités plastiques en élasto-plasticité anisotrope et grandes déformations. Ecole Centrale de Lyon, Lyon
36. Hill R (2001) On the mechanics of localized necking in anisotropic sheet metals. J Mech Phys Solid 49(9):2055–2070
37. Hill R (1991) A theoretical perspective on in-plane forming of sheet metal. J Mech Phys Solid 39(2):295–307
38. Stout MG, Hecker SS (1983) Role of geometry in plastic instability and fracture of tubes and sheet. Mech Mater 2:23–31
39. Ramaekers JAH, Bongaerts PCP (1994) A note on the forming limit curve. In: Shemet'1994, Belfast, UK, pp 39–50
40. Aretz H (2004) Numerical restrictions of the modified maximum force criterion for prediction of forming limits in sheet metal forming. Model Simul Mater Sci Eng 12(4):677–692
41. Banabic D, Comsa DS, Jurco P, Wagner S, He S, Van Houtte P (2004) Prediction of forming limit curves from two anisotropic constitutive models. In: ESAFORM 2004 Conference. Springer, Trondheim, pp 455–459
42. Hutchinson JW, Neale KW, Needleman A (1978) Sheet Necking-I. Validity of plane stress assumptions of the long-wavelength approximation. In: Koistinen DP, Wang NM (eds) Mechanics of sheet metal forming. Plenum, New York, pp 111–126
43. Aretz H (2007) Numerical analysis of diffuse and localized necking in orthotropic sheet metals. Int J Plast 23(5):798–840
44. Banabic D, Aretz H, Paraianu L (2005) Application of various FLD modelling approaches. Model Simul Mater Sci Eng 13:759–769
45. Abspoel M, Scholting ME, Droog JMM (2013) A new method for predicting forming limit curves from mechanical properties. J Mater Process Technol 213(5):759–769
46. Drucker DC (1950) Some implications of work hardening and ideal plasticity. Q Appl Math 7:411–418
47. Hadamard J (1903) Leçons sur la propagation des ondes et les équations de l'hydrodynamiques. Paris
48. Bigoni D, Hueckel T (1991) Uniqueness and localization—associative and non-associative elastoplasticity. Int J Solid Struct 28(2):197–213
49. Neilsen MK, Schreyer HL (1993) Bifurcations in elastic–plastic materials. Int J Solids Struct 30(4):521–544
50. Tvergaard V (1980) Bifurcation and imperfection—sensitivity at necking instabilities. Z Angew Math Mech 60:T26–T34